Exergy analysis of 160 MW three cylinder steam turbine segments

Mrzljak Vedran[1], Poljak Igor[2], Prpić-Oršić Jasna[1], Baressi Šegota Sandi[1]
[1]Faculty of Engineering, University of Rijeka, Vukovarska 58, 51000 Rijeka, Croatia
[2]Department of maritime sciences, University of Zadar, Mihovila Pavlinovića 1, 23000 Zadar, Croatia
E-mail: vedran.mrzljak@riteh.uniri.hr, ipoljak1@unizd.hr, jasna.prpic.orsic@riteh.uniri.hr, sandi.segota@riteh.uniri.hr

Abstract: *Exergy analysis of three cylinder steam turbine segments is performed in this research. The highest mechanical power of 47389.66 kW is developed in the first segment (Seg. I, which actually represents the entire HPC – High Pressure Cylinder). Intermediate Pressure Cylinder (IPC) is the dominant mechanical power producer of all cylinders and it develops 48.95% of cumulative mechanical power produced in the whole turbine. The outlet Low Pressure Cylinder (LPC) segments (Seg. VII and IX) have the highest exergy destructions and the lowest exergy efficiency (equal to 61.27%) of all turbine segments. The best exergy performance shows IPC segments – Seg. V has the lowest exergy destruction (equal to 363.84 kW), while Seg. II has the highest exergy efficiency (equal to 94.04%) of all turbine segments. Outlet LPC segments (Seg. VII and IX) are the most sensitive to the ambient temperature change – their exergy efficiency decreases for 3.19% when the ambient temperature increases from 5 °C to 45 °C.*

KEYWORDS: EXERGY ANALYSIS, COMPLEX STEAM TURBINE, TURBINE SEGMENTS, THE AMBIENT TEMPERATURE CHANGE

1. Introduction

Currently, the majority of electricity worldwide is produced by various kinds of steam turbines [1, 2]. However, steam turbines which can be found in power plants can also be used for many other purposes, the electricity production is a dominant, but not the only task which steam turbine can accomplish [3, 4].

In the conventional thermal or nuclear power plants are used high power steam turbines which are usually composed of several cylinders connected to the same shaft [5, 6]. Medium and low power steam turbines can be composed of one or two cylinders, what depends on the required mechanical power production [7, 8]. Turbine cylinders are usually composed of several turbine stages [9]. However, in exploitation can also be found auxiliary low power steam turbines which are composed of only one Curtis stage (such steam turbines are often used for the pump drive) [10].

Steam turbine cylinders can be single flow or dual flow cylinders, while dual flow cylinders can be symmetrical and dissymmetrical. In single flow turbine cylinder steam expands in just one direction, while in the dual flow cylinder steam expands simultaneously in two directions [11].

This paper presents exergy analysis of a three cylinder steam turbine segments. Such exergy analysis allows insight in the operation of different turbine cylinder parts, the cylinder is not considered as a whole (as in the standard exergy analysis). The observed steam turbine has nine segments overall – produced mechanical power, exergy efficiencies and exergy destructions are presented and compared for all segments. It is also analyzed and observed which turbine segment is the most sensitive to the ambient temperature change.

2. Description and operating regime of the analyzed steam turbine and turbine segments

Observed steam turbine consists of three cylinders which are connected to the same shaft: High Pressure Cylinder (HPC), Intermediate Pressure Cylinder (IPC) and Low Pressure Cylinder (LPC), Fig. 1. HPC and IPC are single flow cylinders, while LPC is a dual flow symmetrical cylinder, therefore both LPC parts (left part LPC-L and right part LPC-R) have the same operating parameters and performance. The shaft on which are connected all cylinders is used for the electric generator drive.

Exergy analysis is performed for all steam turbine segments (what requires division of each cylinder to the segments). Cylinder segment is a part of each cylinder defined between the cylinder inlet, outlet and steam extractions. Each turbine cylinder division to the segments allow insight into the operation performance of different cylinder parts, which cannot be found in the standard plant or turbine exergy analysis [12, 13].

HPC did not possess any steam extractions, therefore HPC has actually only one segment defined between HPC inlet and HPC outlet (HPC is its own segment, Seg. I).

IPC has three steam extractions, which allows IPC division on the four segments. The first IPC segment (Seg. II) is defined between IPC inlet and first IPC extraction (operating point 6, Fig. 1) which deliver a certain steam mass flow rate to the components of high pressure feedwater heating system. Second IPC segment (Seg. III) is defined between first and second IPC extractions (operating points 6 and 7, Fig. 1). Second IPC extraction delivers a certain steam mass flow rate to the deaerator. Third IPC segment (Seg. IV) is defined between second and third IPC extractions (operating points 7 and 8, Fig. 1), where third IPC extraction delivers a certain steam mass flow rate to the components of low pressure condensate heating system. The last, fourth IPC segment (Seg. V) is defined between third IPC extraction and IPC outlet (operating point 9, Fig. 1).

LPC is a dual flow cylinder – steam mass flow rate enters in the cylinder at its central part (operating point 9, Fig. 1) and simultaneously expands through both LPC parts (one half of the steam mass flow rate expands through LPC-L and other half expands through LPC-R). LPC-L and LPC-R have identical steam operating parameters at the inlet, in the extractions and at the outlet which confirms that LPC is symmetrical cylinder (steam temperature, pressure and mass flow rate are identical in operating points 10 and 11 and in operating points 13 and 14, Fig. 1). Each LPC part has two segments which are defined between LPC inlet and steam extraction and between steam extraction and LPC part outlet. For the LPC-L mentioned two segments are marked as Seg. VI and Seg. VII, while for the LPC-R segments are marked as Seg. VIII and Seg. IX. At the end of expansion in both LPC parts (operating points 13 and 14, Fig. 1), remaining steam mass flow rate is delivered to main condenser for condensation [14].

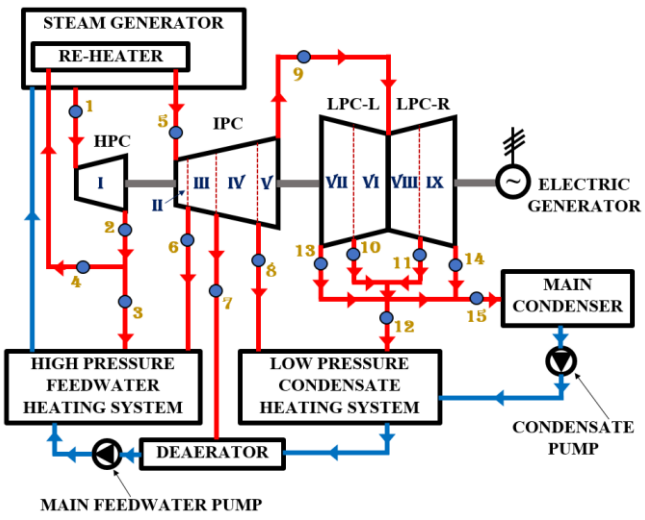

Fig. 1. *General scheme of the three-cylinder 160 MW steam turbine along with operating points required for the exergy analysis and each cylinder marked segments (I – IX)*

Steam expansion process in all cylinders and segments of the observed turbine in Specific enthalpy/Specific entropy (h/s) diagram is shown in Fig. 2. Exergy analysis of any steam turbine cylinder or segment requires data of the real (polytropic) steam expansion process [15]. Data of real expansion process can be properly obtained only from the measurements inside power plant during the exploitation, therefore these data involve all the losses which occur during operation. Losses in the real steam expansion process are proportional to the increase in steam specific entropy, as presented in Fig. 2, so steam specific entropy must continuously increase from the inlet until the outlet of each turbine cylinder or segment. Only in the ideal (isentropic) steam expansion process from the inlet until the outlet of each turbine cylinder or segment, steam specific entropy will remain constant, but the observation of such ideal expansion process is not required in the exergy analysis [16]. It should be highlighted that operating point's numeration and segments marking presented in Fig. 2 are in relation to operating point's numeration and segments marking from Fig. 1.

Steam expansion process is identical in both LPC parts (LPC-L and LPC-R) because LPC is a symmetrical dual flow cylinder, Fig. 2. At the LPC outlet (operating points 13, 14 and 15, Fig. 1 and Fig. 2) steam is slightly under the saturation curve (wet steam) which can be transferred to condensate in main condenser.

Fig. 2 is obtained from known steam operating parameters in each operating point (presented in Table 4) by using NIST-Refprop 9.0 software [17].

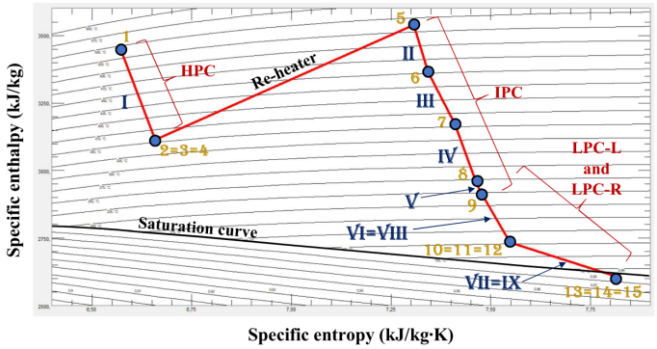

Fig. 2. *Specific enthalpy/Specific entropy (h/s) diagram of steam expansion process throughout steam turbine and all its segments*

3. Exergy analysis equations

In comparison to energy analysis which did not consider parameters of the ambient (ambient pressure and temperature), exergy analysis considers ambient parameters (parameters of the ambient in which observed system, component or component part operates). Second law of thermodynamics is a baseline for an exergy analysis [18, 19].

3.1. Overall equations, balances and principles

During the exergy analysis of any system, component or component part, a few overall equations, balances and principles must always be satisfied [7]. These equations, balances and principles will be presented in this subsection.

The overall exergy balance equation, valid for any system, component or component part at steady state is [9]:

$$\dot{X}_{\text{heat}} - P - \sum \dot{E}x_{\text{outlet}} + \sum \dot{E}x_{\text{inlet}} - \dot{E}x_{\text{Destruction}} = 0, \quad (1)$$

where P is mechanical power. $\dot{E}x$ is a fluid total exergy flow, which can be defined by an equation [8]:

$$\dot{E}x = \dot{m} \cdot \varepsilon, \quad (2)$$

where $\dot{m}$ is a fluid mass flow rate and ε is fluid specific exergy. Fluid specific exergy (ε) is defined by an equation [20]:

$$\varepsilon = (h - h_0) - T_0 \cdot (s - s_0), \quad (3)$$

where h is fluid specific enthalpy, s is fluid specific entropy, T is a temperature and index 0 is related to the ambient state. Exergy transfer by heat at the temperature T ($\dot{X}_{\text{heat}}$) is defined as [6]:

$$\dot{X}_{\text{heat}} = \sum (1 - \frac{T_0}{T}) \cdot \dot{Q}_{\text{heat}}, \quad (4)$$

where $\dot{Q}_{\text{heat}}$ is an energy transfer by heat. Mass flow rate balance for any system, component or component part is [4]:

$$\sum \dot{m}_{\text{inlet}} = \sum \dot{m}_{\text{outlet}}. \quad (5)$$

3.2. Equations for the exergy analysis of turbine segments

Equations for the exergy analysis of the observed turbine segments are defined according to the recommendations from the literature [21-23]. Indexes and segments marking applied in all equations from this subsection are related to the operating points and markings shown in Fig. 1 and Fig. 2. In Table 1 are presented equations for each turbine segment developed mechanical power calculation, while in Table 2 and Table 3 are presented equations for each turbine segment exergy inlet and exergy outlet calculation.

Table 1. *Equations for each segment developed mechanical power calculation*

Segment	Developed mechanical power	Eq.
I	$P_{\text{Seg.I}} = \dot{m}_1 \cdot (h_1 - h_2)$	(6)
II	$P_{\text{Seg.II}} = \dot{m}_5 \cdot (h_5 - h_6)$	(7)
III	$P_{\text{Seg.III}} = (\dot{m}_5 - \dot{m}_6) \cdot (h_6 - h_7)$	(8)
IV	$P_{\text{Seg.IV}} = (\dot{m}_5 - \dot{m}_6 - \dot{m}_7) \cdot (h_7 - h_8)$	(9)
V	$P_{\text{Seg.V}} = (\dot{m}_5 - \dot{m}_6 - \dot{m}_7 - \dot{m}_8) \cdot (h_8 - h_9)$	(10)
VI	$P_{\text{Seg.VI}} = \frac{\dot{m}_9}{2} \cdot (h_9 - h_{10})$	(11)
VII	$P_{\text{Seg.VII}} = (\frac{\dot{m}_9}{2} - \dot{m}_{10}) \cdot (h_{10} - h_{13})$	(12)
VIII	$P_{\text{Seg.VIII}} = \frac{\dot{m}_9}{2} \cdot (h_9 - h_{11})$	(13)
IX	$P_{\text{Seg.IX}} = (\frac{\dot{m}_9}{2} - \dot{m}_{11}) \cdot (h_{11} - h_{14})$	(14)

Table 2. *Equations for each segment exergy inlet calculation*

Segment	Exergy inlet	Eq.
I	$\dot{E}x_{\text{Seg.I,inlet}} = \dot{m}_1 \cdot \varepsilon_1$	(15)
II	$\dot{E}x_{\text{Seg.II,inlet}} = \dot{m}_5 \cdot \varepsilon_5$	(16)
III	$\dot{E}x_{\text{Seg.III,inlet}} = (\dot{m}_5 - \dot{m}_6) \cdot \varepsilon_6$	(17)
IV	$\dot{E}x_{\text{Seg.IV,inlet}} = (\dot{m}_5 - \dot{m}_6 - \dot{m}_7) \cdot \varepsilon_7$	(18)
V	$\dot{E}x_{\text{Seg.V,inlet}} = (\dot{m}_5 - \dot{m}_6 - \dot{m}_7 - \dot{m}_8) \cdot \varepsilon_8$	(19)
VI	$\dot{E}x_{\text{Seg.VI,inlet}} = \frac{\dot{m}_9}{2} \cdot \varepsilon_9$	(20)
VII	$\dot{E}x_{\text{Seg.VII,inlet}} = (\frac{\dot{m}_9}{2} - \dot{m}_{10}) \cdot \varepsilon_{10}$	(21)
VIII	$\dot{E}x_{\text{Seg.VIII,inlet}} = \frac{\dot{m}_9}{2} \cdot \varepsilon_9$	(22)
IX	$\dot{E}x_{\text{Seg.IX,inlet}} = (\frac{\dot{m}_9}{2} - \dot{m}_{11}) \cdot \varepsilon_{11}$	(23)

Table 3. *Equations for each segment exergy outlet calculation*

Segment	Exergy outlet	Eq.
I	$\dot{E}x_{\text{Seg.I,outlet}} = \dot{m}_2 \cdot \varepsilon_2 + P_{\text{Seg.I}}$	(24)
II	$\dot{E}x_{\text{Seg.II,outlet}} = \dot{m}_6 \cdot \varepsilon_6 + (\dot{m}_5 - \dot{m}_6) \cdot \varepsilon_6 + P_{\text{Seg.II}}$	(25)
III	$\dot{E}x_{\text{Seg.III,outlet}} = \dot{m}_7 \cdot \varepsilon_7 + (\dot{m}_5 - \dot{m}_6 - \dot{m}_7) \cdot \varepsilon_7 + P_{\text{Seg.III}}$	(26)
IV	$\dot{E}x_{\text{Seg.IV,outlet}} = \dot{m}_8 \cdot \varepsilon_8 + (\dot{m}_5 - \dot{m}_6 - \dot{m}_7 - \dot{m}_8) \cdot \varepsilon_8 + P_{\text{Seg.IV}}$	(27)
V	$\dot{E}x_{\text{Seg.V,outlet}} = \dot{m}_9 \cdot \varepsilon_9 + P_{\text{Seg.V}}$	(28)
VI	$\dot{E}x_{\text{Seg.VI,outlet}} = \dot{m}_{10} \cdot \varepsilon_{10} + (\frac{\dot{m}_9}{2} - \dot{m}_{10}) \cdot \varepsilon_{10} + P_{\text{Seg.VI}}$	(29)
VII	$\dot{E}x_{\text{Seg.VII,outlet}} = \dot{m}_{13} \cdot \varepsilon_{13} + P_{\text{Seg.VII}}$	(30)
VIII	$\dot{E}x_{\text{Seg.VIII,outlet}} = \dot{m}_{11} \cdot \varepsilon_{11} + (\frac{\dot{m}_9}{2} - \dot{m}_{11}) \cdot \varepsilon_{11} + P_{\text{Seg.VIII}}$	(31)
IX	$\dot{E}x_{\text{Seg.IX,outlet}} = \dot{m}_{14} \cdot \varepsilon_{14} + P_{\text{Seg.IX}}$	(32)

Exergy destruction of each turbine segment is calculated as:

$$\dot{E}x_{\text{Seg.(i),Destruction}} = \dot{E}x_{\text{Seg.(i),inlet}} - \dot{E}x_{\text{Seg.(i),outlet}}. \quad (33)$$

Each turbine segment exergy efficiency is calculated as:

$$\eta_{\text{Seg.(i),EX}} = \frac{P_{\text{Seg.(i)}}}{\dot{E}x_{\text{Seg.(i),inlet}} - \dot{E}x_{\text{Seg.(i),outlet}} + P_{\text{Seg.(i)}}}. \quad (34)$$

In Eq. 33 and Eq. 34 index i represents each turbine segment (i = I, II, III, IV, V, VI, VII, VIII and IX).

4. Steam operating parameters required for the turbine segments exergy analysis

Exergy analysis of each observed turbine segment is performed by using steam operating parameters measured in each operating point (Fig. 1 and Fig. 2) during the plant exploitation. These operating parameters are found in [24] and presented in Table 4. During the plant exploitation, in each operating point from Fig. 1 and Fig. 2 are measured steam temperature, pressure and mass flow rate - other steam operating parameters presented in Table 4 are calculated using NIST-Refprop 9.0 software [17].

As the exergy analysis considers parameters of the ambient (ambient temperature and pressure), in exergy analysis of any system, component or segment is required the definition of the base ambient state [25]. In this research, the base ambient state is defined by the ambient temperature of 25 °C and the ambient pressure of 1 bar.

Table 4. *Steam operating parameters for the turbine segments exergy analysis*

O. P. *	Temp. (°C)	Pressure (bar)	Mass flow rate (kg/s)	Specific enthalpy (kJ/kg)	Specific entropy (kJ/kg·K)	Specific exergy (kJ/kg) **
1	538	129.19	145.10	3440.6	6.5738	1485.20
2	355	36.33	145.10	3114.0	6.6586	1133.30
3	355	36.33	10.10	3114.0	6.6586	1133.30
4	355	36.33	135.00	3114.0	6.6586	1133.30
5	538	32.39	135.00	3540.3	7.3062	1366.60
6	452	18.04	7.60	3365.2	7.3429	1180.40
7	356	8.37	7.44	3174.1	7.4091	969.63
8	244	3.20	8.01	2955.0	7.4638	734.21
9	226	2.69	111.95	2920.3	7.4747	696.26
10	128	0.92	2.35	2733.5	7.5482	487.54
11	128	0.92	2.35	2733.5	7.5482	487.54
12	128	0.92	4.70	2733.5	7.5482	487.54
13	65	0.25	53.63	2610.4	7.8094	286.61
14	65	0.25	53.63	2610.4	7.8094	286.61
15	65	0.25	107.25	2610.4	7.8094	286.61

* O. P. = Operating Point (according to Fig. 1 and Fig. 2)
** At the base ambient state

5. Results and discussion

Developed mechanical power in each segment of the analyzed steam turbine, which is one of the essential parameters in the exergy analysis of any turbine segment, is presented in Fig. 3.

Observing all segments, it can easily be concluded that the highest mechanical power of 47389.66 kW is developed in the first segment (Seg. I, which actually represents the entire HPC). Each of the first three IPC segments (Seg. II, III and IV) develop notable mechanical power, while the last IPC segment (Seg. V) develop the lowest mechanical power of all turbine segments, Fig. 3. Low pressure steam turbine cylinder is symmetrical one, therefore both LPC parts (LPC-L and LPC-R) develop the same mechanical power. Symmetrical LPC segments (Seg. VI and VIII, as well as Seg. VII and IX) also develop identical mechanical power.

In three cylinder steam turbines, LPC is usually the dominant mechanical power producer [13]. Steam turbine analyzed in this paper strongly deviates from this general guideline. In the observed steam turbine, IPC is the dominant mechanical power producer of all cylinders and it develops 48.95% of cumulative mechanical power produced in the whole turbine. HPC develops 29.68%, while LPC (both LPC parts) develops only 21.37% of cumulative mechanical power produced in the whole turbine.

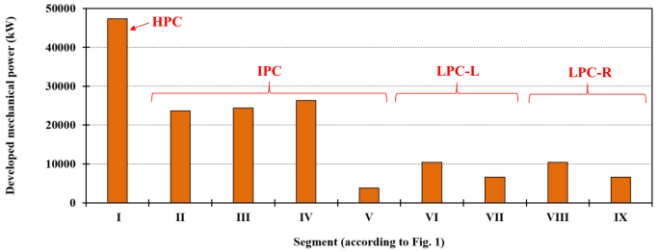

Fig. 3. *Developed mechanical power in each segment of the analyzed steam turbine*

Exergy destruction and exergy efficiency of each steam turbine segment at the base ambient state are presented in Fig. 4.

The outlet LPC segments (Seg. VII and IX) have the highest exergy destructions and the lowest exergy efficiency (equal to 61.27%) of all turbine segments. At least some turbine stages in the LPC outlet segments operate with wet steam (water droplets in wet steam increase losses) and in supersonic regime, so high exergy destruction and low exergy efficiency of the outlet LPC segments can be expected. The best exergy performance shows IPC segments – Seg. V has the lowest exergy destruction (equal to 363.84 kW), while Seg. II has the highest exergy efficiency (equal to 94.04%) of all turbine segments. HPC (Seg. I) has high exergy destruction, just slightly lower than outlet LPC segments, however such high exergy destruction did not notably ruin its exergy efficiency (Seg. I exergy efficiency is equal to 92.81%).

Considering turbine cylinders, in three cylinder steam turbines IPC usually shows the best performance (because IPC did not operate with the steam of the highest pressure in the plant as HPC and neither one IPC stage did not operate with wet steam as occur in some LPC outlet stages) [4, 13]. For the observed steam turbine, it can be concluded that HPC and IPC shows very similar exergy performance, so clear dominance of the IPC in relation to other cylinders did not exist for steam turbine analyzed in this paper.

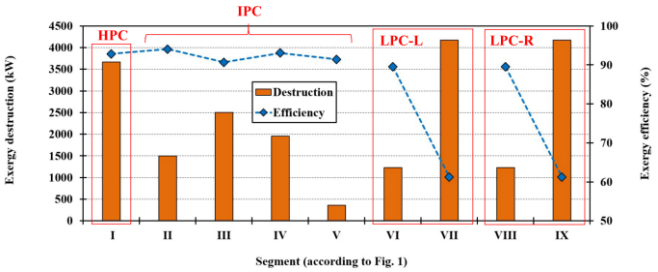

Fig. 4. *Exergy destruction and exergy efficiency of each analyzed steam turbine segment at the base ambient state*

Final part of the observed steam turbine segments research was related to each segment sensitivity on the ambient temperature change. During the ambient temperature variation, the ambient pressure remains always the same and identical as at the base ambient state. For each segment is valid a conclusion that increase in the ambient temperature simultaneously increases segment exergy destruction and decrease segment exergy efficiency. However, the intensity of exergy destruction and exergy efficiency change during the ambient temperature variation differs from one turbine segment to another.

Decrease in exergy efficiency of each steam turbine segment during the ambient temperature increase from 5 °C to 45 °C is presented in Fig. 5. From Fig. 5 is clear that LPC is much more sensitive to the ambient temperature change in comparison to other two cylinders. Outlet LPC segments (Seg. VII and IX) are the most sensitive to the ambient temperature change – their exergy efficiency decreases for 3.19% when the ambient temperature increases from 5 °C to 45 °C. Seg. II of the IPC is the least sensitive to the ambient temperature change – increase in the ambient temperature from 5 °C to 45 °C decreases Seg. II exergy efficiency for 0.71% only.

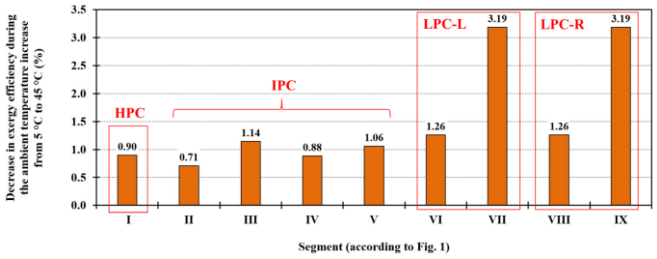

Fig. 5. Decrease in exergy efficiency of each steam turbine segment during the ambient temperature increase from 5 °C to 45 °C

6. Conclusions

Exergy analysis of complex three cylinder steam turbine segments is performed in this paper. The most important conclusions are:

- The highest mechanical power of 47389.66 kW is developed in the first segment (Seg. I, which actually represents the entire HPC).
- In the observed steam turbine, IPC is the dominant mechanical power producer of all cylinders and it develops 48.95% of cumulative mechanical power produced in the whole turbine. HPC develops 29.68%, while LPC (both LPC parts) develops only 21.37% of cumulative mechanical power produced in the whole turbine.
- The outlet LPC segments (Seg. VII and IX) have the highest exergy destructions and the lowest exergy efficiency (equal to 61.27%) of all turbine segments.
- The best exergy performance shows IPC segments – Seg. V has the lowest exergy destruction (equal to 363.84 kW), while Seg. II has the highest exergy efficiency (equal to 94.04%) of all turbine segments.
- HPC (Seg. I) has high exergy destruction, just slightly lower than outlet LPC segments, but sufficiently high exergy efficiency (Seg. I exergy efficiency is equal to 92.81%).
- LPC is much more sensitive to the ambient temperature change in comparison to other two cylinders (HPC and IPC).
- Outlet LPC segments (Seg. VII and IX) are the most sensitive to the ambient temperature change – their exergy efficiency decreases for 3.19% when the ambient temperature increases from 5 °C to 45 °C.

7. Acknowledgment

This research has been fully supported by the Croatian Science Foundation under the project IP-2022-10-2821.

8. References

[1] Tanuma, T. (Ed.). (2017). Advances in steam turbines for modern power plants. Woodhead Publishing.

[2] Giampaolo, T. (2020). Gas turbine handbook: principles and practice. River Publishers.

[3] Anđelić, N., Lorencin, I., Mrzljak, V., & Car, Z. (2024). On the application of symbolic regression in the energy sector: Estimation of combined cycle power plant electrical power output using genetic programming algorithm. Engineering applications of artificial intelligence, 133, 108213. (doi:10.1016/j.engappai.2024.108213)

[4] Poljak, I., & Mrzljak, V. (2023). Thermodynamic Analysis and Comparison of Two Marine Steam Propulsion Turbines. NAŠE MORE: znanstveni časopis za more i pomorstvo, 70(2), 0-0. (doi:10.17818/NM/2023/2.2)

[5] Elhelw, M., Al Dahma, K. S., & el Hamid Attia, A. (2019). Utilizing exergy analysis in studying the performance of steam power plant at two different operation mode. Applied Thermal Engineering, 150, 285-293. (doi:10.1016/j.applthermaleng.2019.01.003)

[6] Mrzljak, V., Anđelić, N., Lorencin, I., & Sandi Baressi Šegota, S. (2021). The influence of various optimization algorithms on nuclear power plant steam turbine exergy efficiency and destruction. Pomorstvo, 35(1), 69-86. (doi:10.31217/p.35.1.8)

[7] Aljundi, I. H. (2009). Energy and exergy analysis of a steam power plant in Jordan. Applied thermal engineering, 29(2-3), 324-328. (doi:10.1016/j.applthermaleng.2008.02.029)

[8] Poljak, I., Mrzljak, V., Senčić, T., & Pastorčić, D. (2024). Isentropic and exergy analyses of marine steam turbine segments at several loads. Scientific Journal of Maritime Research-Pomorstvo, 38(1). (doi:10.31217/p.38.1.8)

[9] Kaushik, S. C., Reddy, V. S., & Tyagi, S. K. (2011). Energy and exergy analyses of thermal power plants: A review. Renewable and Sustainable energy reviews, 15(4), 1857-1872. (doi:10.1016/j.rser.2010.12.007)

[10] Mrzljak, V., Prpić-Oršić, J., & Poljak, I. (2018). Energy power losses and efficiency of low power steam turbine for the main feed water pump drive in the marine steam propulsion system. Pomorski zbornik, 54(1), 37-51. (doi:10.18048/2018.54.03)

[11] Kostyuk, A., & Frolov, V. (1988). Steam and gas turbines. Mir Publishers.

[12] Koroglu, T., & Sogut, O. S. (2018). Conventional and advanced exergy analyses of a marine steam power plant. Energy, 163, 392-403. (doi:10.1016/j.energy.2018.08.119)

[13] Mrzljak, V., Jelić, M., Poljak, I., & Prpić-Oršić, J. (2023). Analysis and Comparison of Main Steam Turbines from Four Different Thermal Power Plants. Pomorstvo, 37(1), 58-74. (doi:10.31217/p.37.1.6)

[14] Mrzljak, V., Prpić-Oršić, J., Poljak, I., & Šegota, S. B. (2020). Exergy analysis of steam condenser at various loads during the ambient temperature change. Machines. Technologies. Materials., 14(1), 12-15.

[15] Zhao, Z., Su, S., Si, N., Hu, S., Wang, Y., Xu, J., ... & Xiang, J. (2017). Exergy analysis of the turbine system in a 1000 MW double reheat ultra-supercritical power plant. Energy, 119, 540-548. (doi:10.1016/j.energy.2016.12.072)

[16] Medica-Viola, V., Baressi Šegota, S., Mrzljak, V., & Štifanić, D. (2020). Comparison of conventional and heat balance based energy analyses of steam turbine. Pomorstvo, 34(1), 74-85. (doi:10.31217/p.34.1.9)

[17] Lemmon, E. W., Huber, M. L., & McLinden, M. O. (2010). NIST Standard Reference Database 23, Reference Fluid Thermodynamic and Transport Properties (REFPROP), version 9.0, National Institute of Standards and Technology. R1234yf. fld file dated December, 22, 2010.

[18] Kanoğlu, M., Çengel, Y. A. & Dincer, I. (2012). Efficiency Evaluation of Energy Systems. Springer Briefs in Energy. (doi:10.1007/978-1-4614-2242-6)

[19] Mrzljak, V., Jelić, M., Poljak, I., & Medica-Viola, V. (2023). Exergy analysis of supercritical CO2 system for marine diesel engine waste heat recovery application. Pomorski zbornik, 63, 39-62.

[20] Tan, H., Shan, S., Nie, Y., & Zhao, Q. (2018). A new boil-off gas re-liquefaction system for LNG carriers based on dual mixed refrigerant cycle. Cryogenics, 92, 84-92. (doi:10.1016/j.cryogenics.2018.04.009)

[21] Baressi Šegota, S., Lorencin, I., Anđelić, N., Mrzljak, V., & Car, Z. (2020). Improvement of marine steam turbine conventional exergy analysis by neural network application. Journal of Marine Science and Engineering, 8(11), 884. (doi:10.3390/jmse8110884)

[22] Erdem, H. H., Akkaya, A. V., Cetin, B., Dagdas, A., Sevilgen, S. H., Sahin, B., ... & Atas, S. (2009). Comparative energetic and exergetic performance analyses for coal-fired thermal power plants in Turkey. International Journal of Thermal Sciences, 48(11), 2179-2186. (doi:10.1016/j.ijthermalsci.2009.03.007)

[23] Mrzljak, V., Poljak, I., Jelić, M., & Prpić-Oršić, J. (2023). Thermodynamic Analysis and Improvement Potential of Helium Closed Cycle Gas Turbine Power Plant at Four Loads. Energies, 16(15), 5589. (doi:10.3390/en16155589)

[24] Tavana, M., Deymi-Dashtebayaz, M., Dadpour, D., & Mohseni-Gharyehsafa, B. (2023). Realistic energy, exergy, and exergoeconomic (3E) characterization of a steam power plant: multi-criteria optimization case study of mashhad tous power plant. Water, 15(17), 3039. (doi:10.3390/w15173039)

[25] Mrzljak, V., Poljak, I., & Žarković, B. (2018). Exergy analysis of steam pressure reduction valve in marine propulsion plant on conventional LNG carrier. NAŠE MORE: znanstveni časopis za more i pomorstvo, 65(1), 24-31. (doi:10.17818/NM/2018/1.4)